Journal of Computer Science & Computational Mathematics, Volume 6, Issue 3, September 2016
DOI: 10.20967/jcscm.2016.03.007

Analysis of Fourier and Non-Fourier heat conduction using Tiknonov based Well-conditioned Asymptotic Waveform Evaluation Technique

Sohel Rana[1], Ahmed Wasif Reza[2*], Mohd Sayuti[3]

[1]School of Engineering, RMIT University,
[2]Department of Computer Science and Engineering, Faculty of Science and Engineering, East West University,
[3]Department of Mechanical Engineering, Faculty of Engineering, University of Malaya,
[*]Corresponding author email: wasif@ewubd.edu, awreza98@yahoo.com

***Abstract*:** The unprecedented success of information technology has been focused by semiconductor industry to advance at dramatic rate. Thermal issues are hastily becoming one of the most challenging problems in high-performance chip design due to ever-increasing device. In the analysis of heat transport of IC chip, Fourier's heat conduction mechanism was frequently used. It is known that, this equation suggests a presumption of infinite thermal propagation speed. Then non-Fourier heat conduction model was used to forecast the rapid transient heat conduction process. A number of traditional iterative and moments matching based solvers can be found to analyze the Fourier and non-Fourier heat conduction model such as Runge-Kutta (RK) and Asymptotic Waveform Evaluation (AWE) technique. The iteration based RK method is computationally expensive and the AWE moment matching is inherently ill-conditioned. In present work, Tiknonov based Well-conditioned Asymptotic Waveform Evaluation (TWCAWE) technique has proposed to analyze the Fourier and non-Fourier heat conductions. The TWCAWE technique is successfully able to avoid the ill-conditioning moment matching and also 1.2 times faster compared to AWE.

***Keywords*:** Fourier and non-Fourier, TWCAWE, heat conduction.

1. Introduction

The increasing demand for higher performance in integrated circuits (ICs) results in faster switching speed, greater number of transistors , increased functional density and large chip size. The growing demand for additional multifaceted VLSI circuits with higher performance is leading to higher power dissipation and enlarged the thermal problems. So, thermal management is vital to the growth of upcoming generations of microprocessors, integrated network processors, and systems-on-a chip. A large amount of research can be found in the field of the thermal analysis of IC chips and its packaging on the background of thermal reliability. In the analysis of heat transport of IC chip, Fourier's heat conduction equation mechanism was frequently used. In some situations involving temperature near absolute zero, extreme thermal gradients, and high heat flux conduction, short time behavior Fourier's law is invalid [1, 2]. So, an analysis of no-Fourier heat conduction in IC chip has become important in recent years. A number of traditional iterative and moment-matching based solvers can be found to analyze the Fourier and non-Fourier heat conduction models. In the case of heat transfer problem, iteration based Runge-Kutta (RK) method is very well known and the results obtained from RK are accurate [3]. But, RK technique is computationally expensive [2, 3]. To reduce the computational time, moment matching based technique known as Asymptotic Waveform Evaluation (AWE) method was introduced [3]. AWE technique is able to solve one dimensional, two dimensional and three-dimensional models [4]. The limitation of AWE model is that the model cannot forecast the temperature responses accurately as it is ill-conditioned moment matching [5-8].

In this study, we have proposed a Tiknonov based Well-conditioned Asymptotic Waveform Evaluation (TWCAWE) method to investigate the Fourier and non-Fourier heat conduction implanted with Tickhonov regularization technique to enrich the immovability [9-11]. In this proposed TWCAWE model, there is no need to renovate non-Fourier heat conduction equation into linear equation. The results obtained from TWCAWE method precisely matched with Runge-Kutta (R-K) results and also competents to remove all instabilities of AWE. Additionally, the method proposed in the current work is 1.2 times faster compared to AWE.

2. Mathematical Model

The fundamental perception of the Fourier heat conduction model is infinite thermal wave propagation speed. The classical Fourier heat conduction law relates the heat flux vector q to the temperature gradient $\nabla\theta$, as in (1).

$$q = -K_c \nabla \theta \tag{1}$$

where K_c is thermal conductivity.
Hence, the above traditional parabolic heat equation is symbolized by (2) that originated from (1).

$$\sigma \nabla \theta = \frac{\partial \theta}{\partial t} \tag{2}$$

Here, $\sigma = K_c/\rho c$, ρ and c are thermal diffusivity, mass density and specific heat capacity, respectively.

The traditional heat conduction equation symbolized by (1), which is unable to explain some distinct cases of heat conduction, e.g., near the absolute zero temperature and extreme thermal gradient. D. Y. Tzou [3] suggested a non-Fourier heat transfer model that contains two phases of delay denoted by (3). Due to the presence of phase delay, this model is able to describe these distinct situations and also is able to eradicate the dimness of the classical heat conduction model.

$$Q(r,t+\kappa_a) = -K_c \nabla \theta(r,t+\kappa_b) \tag{3}$$

where κ_b is the phase delay of longitudinal temperature gradient in regards to local temperature and κ_a is the phase delay of heat flux in regards to local temperature.

The model denoted by (3) promises both phase delay κ_a and κ_b for fast heat transfer. The model is represented in a standardized two-dimensional hyperbolic equation specified by (4).

$$\frac{\partial^2 \phi}{\partial \varepsilon^2} + \frac{\partial^2 \phi}{\partial \psi^2} + Z_b \frac{\partial^3 \phi}{\partial \beta \partial \varepsilon^2} + Z_b \frac{\partial^3 \phi}{\partial \beta \partial \psi^2} = \frac{\partial \phi}{\partial \beta} + Z_a \frac{\partial^2 \phi}{\partial \beta^2} \tag{4}$$

where,

$$\phi = \frac{\theta - \theta_0}{\theta_w - \theta_0},\ \beta = \frac{t}{l^2/\sigma},\ \varepsilon = \frac{x}{l},\ \psi = \frac{y}{h},\ Z_a = \frac{\kappa_a}{l^2/\sigma},\ Z_b = \frac{\kappa_b}{l^2/\sigma}$$

Here, β is standardized time, Z_b is standardized phase delay for temperature gradient, and Z_a is standardized phase delay for heat flux. The length and width are given by *l* and *h*, correspondingly, while σ is the thermal diffusivity.

Finite element model (FEM) is a sturdy technique as it is able to explain multi-dimensional and diverse types of problems. FEM meshing was carried out using the rectangular element with nodes *j, k,m* and *o*. FEM based on Galerkin's weighted residual technique is applied on (4) to achieve (5) .

$$\begin{aligned} &[N]^T \frac{\partial \varphi}{\partial \varepsilon}\Big|_j^k + [N]^T \frac{\partial \varphi}{\partial \psi}\Big|_k^m + Z_b [N]^T \frac{\partial \dot{\varphi}}{\partial \varepsilon}\Big|_j^k + \\ &Z_b [N]^T \frac{\partial \dot{\varphi}}{\partial \psi}\Big|_k^m - \int_j^k \frac{\partial [N]^T}{\partial \varepsilon} \frac{\partial \varphi}{\partial \varepsilon} dA - \int_k^m \frac{\partial [N]^T}{\partial \psi} \frac{\partial \varphi}{\partial \psi} dA \\ &- \int_j^k Z_b \frac{\partial [N]^T}{\partial \varepsilon} \frac{\partial \dot{\varphi}}{\partial \varepsilon} dA - \int_k^m Z_b \frac{\partial [N]^T}{\partial \psi} \frac{\partial \dot{\varphi}}{\partial \psi} dA - \\ &\int_j^k (N_K \dot{\varphi} + Z_a N_K \ddot{\varphi}) d\zeta d\zeta = 0 \end{aligned} \tag{5}$$

Elemental matrices can be instigated for any type of model by using(5).

2.1 TWCAWE algorithm

Consider a model of physical phenomenon

$$K(s)x(s) = F(s) \tag{6}$$

where *K*(*s*) is the compound matrix, *F*(*s*) is the compound excitation vector, *x*(*s*) is the key vector and *s=j2πf.*

Consider an extension point s_0($s_0=j2\pi f_0$) and the Taylor series is [5],

$$\sum_{n=0}^{b_1} (s-s_0)^n K_n x(s) = \sum_{n=0}^{c_1} (s-s_0)^n F_n \tag{7}$$

where b_1 and c_1 are selected large enough so that no substantial higher order terms of K_n and/or F_n are trimmed.

The moments matching AWE subspaces for (7) are rendering to (8), the moments are as follows

$$\begin{aligned} \hat{m}_1 &= K_0^{-1} F_0 \\ \hat{m}_2 &= K_0^{-1}(F_1 - K_1 \hat{m}_1) \\ \hat{m}_3 &= K_0^{-1}(F_2 - K_2 \hat{m}_2) \\ &\vdots \\ \hat{m}_q &= K_0^{-1}(F_{q-1} - \sum_{d=1}^{q-1} K_d \hat{m}_{q-d}) \end{aligned} \tag{8}$$

The above moments are linearly dependent for trivial values of *q* as monotonous pre-multiplied by K_0^{-1} To avoid these difficulties, moments are calculated in an alternative way in TWCAWE method which is able to produce significant results for any values of *q*. Consider TWCAWE moment subspaces are $\hat{V} = (\hat{v}_1, \hat{v}_2, ..., \hat{v}_n)$ The TWCAWE moments (Algorithm 1) are calculated, as shown in below Table 1.

Table 1. Algorithm 1(TWCAWE moments calculation)

1	$\hat{v}_1 = K_0^{-1} F_0$
2	$Z_{[1,1]} = \|\hat{v}_1\|$
3	$\hat{w}_1 = \hat{v} Z_{[1,1]}^{-1}$
4	for *r*=2,3,…,*n*
5	$\hat{v}_r = K_0^{-1}\left(\sum_{m=1}^{r-1}\left(F_m e_1^T J_{U_1}(r,m) - K_1 \hat{w}_{r-1} - \sum_{m=2}^{r-1} K_m \hat{w}_{r-m} J_{U_2}(r,m) e_{r-m}\right)\right)$
6	for *p*=1,2,3,…,(*r*-1) do
7	$Z_{[p,r]} = \hat{w}_p^H \hat{v}_r$
8	$\hat{v}_n = \hat{v}_n - Z_{[p,r]} \hat{w}_p$
9	$Z_{[r,r]} = \|\hat{v}_r\|, \hat{w}_r = \hat{v}_r Z_{[r,r]}^{-1}$

Here, we simplified certain scheme:

$$J_{U_w}(r,m) = \prod_{i=1}^{m} Z_{[i:r-m+i-1, i:r-m+i-1]}$$

And, e_r is the r^{th} unit vector; all its entries are 0 excluding the r^{th}, which is 1.

2.2 Tikhonov scheme

TWCAWE algorithm implements the Tikhonov regularization technique [9] to amend the stiffness matrix marginally in mandate to condense the volatility problem. Contemplate a well-condition approximation problem, $Kx \approx y$, the residual $\|Kx - y\|_2$ appears to be the minimum depending on the optimal of $x = (K*K)^{-1} K*y$. The singularity complaint of $(K*K)^{-1}$ can be condensed by adding a term, which is indicated in (9)

$$x = (K*K + h_c^2 I)^{-1} K*y \tag{9}$$

Here, h_c is the regulation parameter which depends on the order of the equation, whereas *I* is the identical matrix. The family of this estimated inverse is defined by $C_h = (K*K + h_c^2 I)^{-1} K$. In TWCAWE, during moment calculation, inverse of K_0 matrix is supernumerary by C_h

from WCAWE algorithm. Particulars of h_c and I can be found at [9].

2.3 Transient response

The nodal moments [a] can be taken out from the global moment matrix for any random node i,

$$\left[a_n\right]_i = \left[\hat{V}\right]_i \tag{10}$$

The transient response for any random node i can be approximated by using Pade approximation, then supplementary streamlined to partial fractions [3], as exposed in (11)-(13).

$$T_i(s) = a_0 + a_1 s + a_2 s^2 + . \quad . \quad . + a_n s^n \tag{11}$$

$$= \frac{\mathrm{d}_0 + \mathrm{d}_1 \mathrm{s} + \ldots + \mathrm{d}_{\mathrm{s-1}} \mathrm{s}^{\mathrm{s-1}}}{1 + \mathrm{c}_1 \mathrm{s} + \ldots + \mathrm{c}_\mathrm{s} \mathrm{s}^\mathrm{s}} \tag{12}$$

$$= \frac{r_1}{s - p_1} + \frac{r_2}{s - p_2} + . \ . \ . + \frac{r_q}{\mathrm{s\text{-}p}_q} \tag{13}$$

Poles and Residues can be originated by resolving (14)-(16).

$$\begin{bmatrix} a_0 & a_1 & a_2 \ldots & .a_{q-1} \\ a_1 & a_2 & a_3 .. & .a_q \\ .. & . . . & . \ . \ . & . \ . \\ . & . \ . \ . \ . & . \ . \ . & . \\ a_{q-1} & . \ . \ . \ . \ . \ . & . \ . & a_{2q-2} \end{bmatrix} \begin{bmatrix} c_q \\ c_{q-1} \\ . \\ . \\ c_1 \end{bmatrix} = - \begin{bmatrix} a_q \\ a_{q-1} \\ . \\ . \\ a_1 \end{bmatrix} \tag{14}$$

$$??? \sum_{i=1}^{r} c_i p^i + 1 = 0 \tag{15}$$

$$\begin{bmatrix} p_1^{-1} & p_2^{-1} & p_3^{-1} & . & p_q^{-1} \\ p_1^{-2} & p_2^{-2} & p_3^{-2} & . & p_q^{-2} \\ . & . & . & & \\ . & . & . & . & . \\ p_1^{-s} & p_2^{-s} & p_3^{-s} & . & p_q^{-q} \end{bmatrix} \begin{bmatrix} r_1 \\ r_2 \\ . \\ . \\ r_q \end{bmatrix} = - \begin{bmatrix} a_0 \\ a_1 \\ . \\ . \\ a_{q-1} \end{bmatrix} \tag{16}$$

The final transient response for any random node, i is

$$T_i(t) = \sum_{i=1}^{q} \frac{r_i^*}{p_i^*} \left[\left\{ e^{real(p_i^*)} \left(\cos(imag(p_i^*))t + \sin(imag(p_i^*))t \right) \right\} - 1 \right] \tag{17}$$

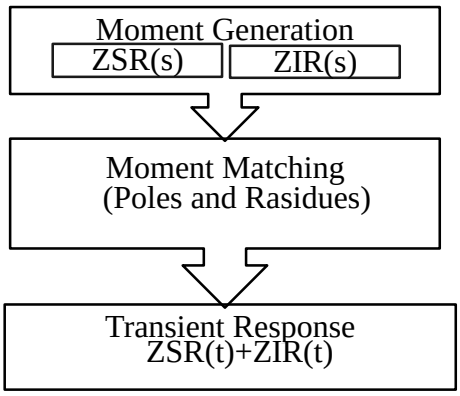

Figure 1. Flow chart of TWCAWE moment calculation

3. Results and Discussion

3.1 Observation of Fourier heat conduction

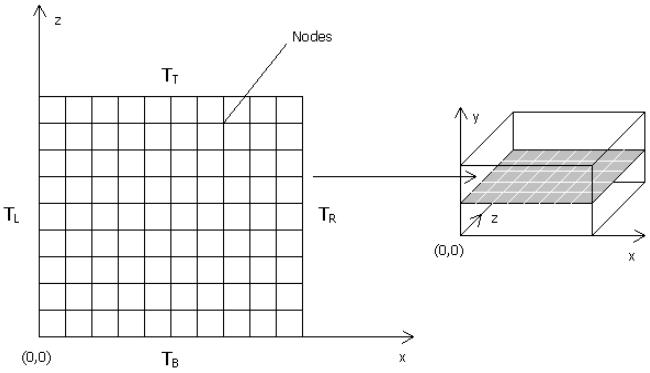

Figure 32. Schematic of two dimensional heat conduction models

Figure 2 shows the rectangular slab with instantaneous temperature imposed left edge of the slab. Figure 3 and Figure 4 exemplify the Fourier temperature responses respecting normalized time and normalized distance correspondingly with instant heat imposed left edge of the boundary. The results demonstrate that, the thermal influence is sensed instantaneously throughout the system if the surface of a material is heated. This leads to simultaneous development of heat flux and temperature gradient. Classical Fourier low assumes that instantaneous thermal equilibrium between electron and phonons. Figure 3 and Figure 4 also spectacles that, when instantaneous heat executed left edge of the boundary the same thermal effect felt right edge of the slab instantly.

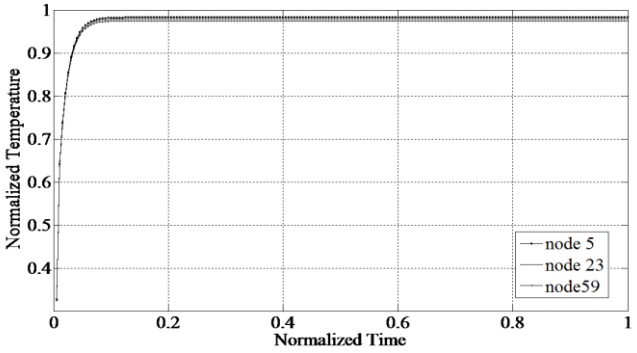

Figure 3. Normalized temperature responses for Fourier heat conduction

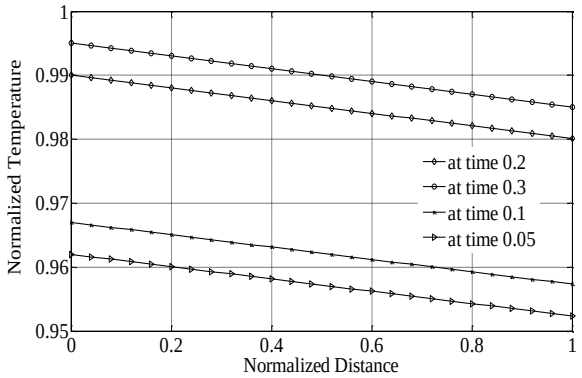

Figure 4. Fourier temperature responses along the centre of the slab for different time

3.2 Non-Fourier heat conduction

Figures 5-7 show the temperature distribution for above rectangular slab considering different values of Z_b as 0.5, 0.05 and 0.0001, respectively. The temperature spectrum shown in Figures 5-7 are plotted by considering the node situated middle of the slab, all the responses are calculated by TWCAWE method. It is clear from the figure that, all temperature responses are continuous and accurate for different values of Z_b. In this scheme, the individual poles and residues are used to calculate the individual temperature responses. So, this scheme is accurately predict temperature distribution along the system. The initial high frequency and delay due to relaxation time of electron are clear in Figure 7 for Z_b=0.0001.

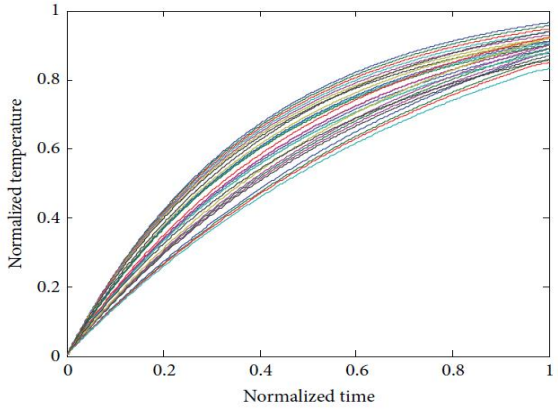

Figure 5. Normalized temperature response spectrum along centre of the slab in the case of Z_b=0.5

Figure 8 (a) and Figure 8 (b) display the temperature spreading of sudden heat executed on the left edge of the slab, the figures also signify the comparison of TWCAWE, R-K and AWE methods for diverse values of Z_b at node 5 and node 59, respectively. It can be observed that, at node 5, initial fluctuation has been reduced, this helps to approximate the temperature behavior of other node accurately (e.g., node 59), as shown in Figure 8.

This evaluation spectacles that, TWCAWE results absolutely match with the R-K outcome for Z_b=0.5 and 0.05, but AWE results show inconsistency. For the instance of Z_b=0.0001, TWCAWE congregates to similar steady state as R-K. Before uniting to the steady-state, R-K results display convergence with TWCAWE, but AWE is incompetent to forecast the accurate temperature response as TWCAWE and R-K due to instability of AWE. It can also be observed from Figure 5 that, for TWCAWE method, the temperature behaviours are converged after normalized time of 0.25 and 0.31 in case of Z_b=0.05 and Z_b=0.0001, respectively at node 5. In case of node 59, the temperature behaviours are converged after normalized time of 0.5 and 0.9 for Z_b=0.05 and Z_b=0.0001, respectively; because the node 59 is far from the boundary where temperature is imposed.

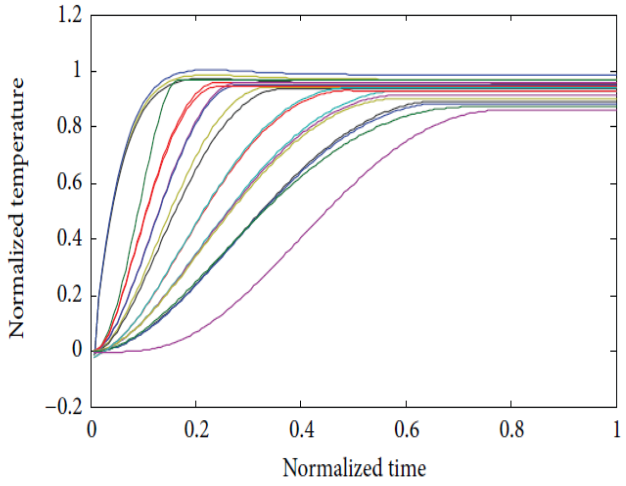

Figure 6. Normalized temperature response spectrum along centre of the slab in the case of Z_b=0.05

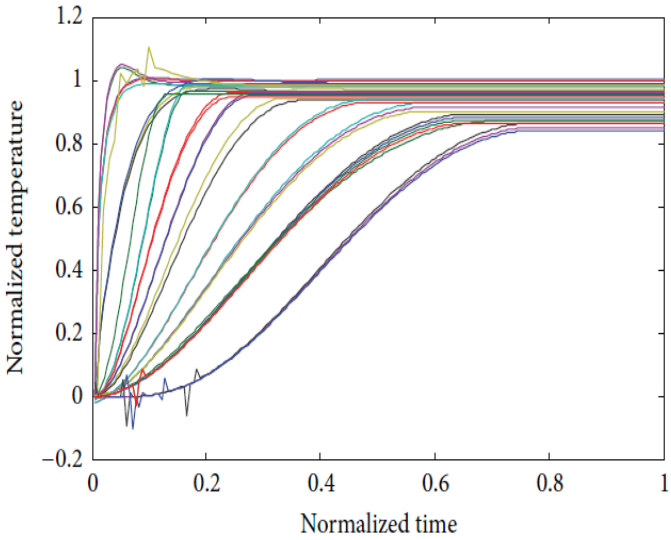

Figure 7. Normalized temperature response spectrum along centre of the slab for the case of Z_b=0.0001

Figures 9(a), 9(b), 9(c) and 9(d) display the non–Fourier temperature circulation respecting distance along the centre of the slab at time 0.005, 0.05, 0.1 and 0.5, correspondingly for TWCAWE. This temperature distribution with instant heat executed at boundary conditions for Z_b=0.5, 0.05 and 0.0001. Immediate heat pulse is imposed on the left edge of the slab and the heat is drifting towards the other edge of the slab. Figure 9 also shows the evaluation of TWCAWE, R-K and AWE outcomes. The evaluation shows the TWCAWE results precisely adjacent to R-K solution, but AWE shows inconsistency.

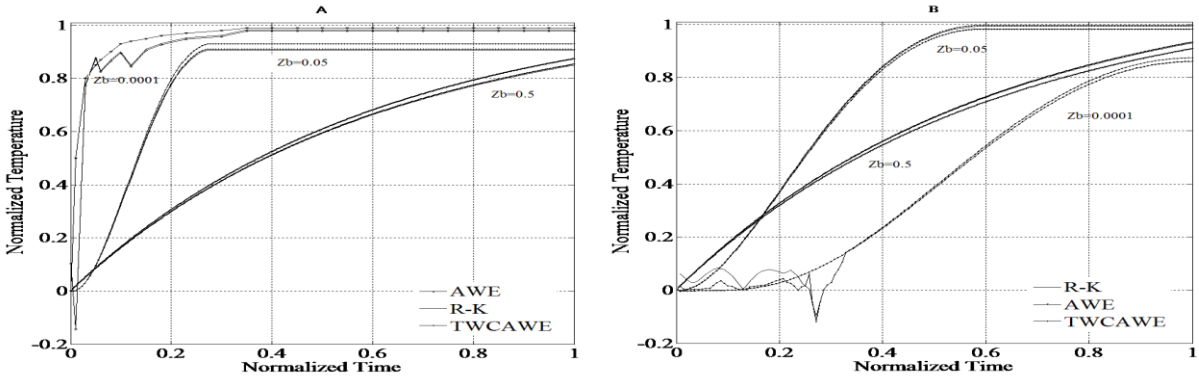

Figure 8. Normalized temperature responses along the Centre of the slab for Z_b=0.5, 0.05 and for Z_b=0.0001 with instantaneous heat imposed, (a) at node 5, (b) at node 59

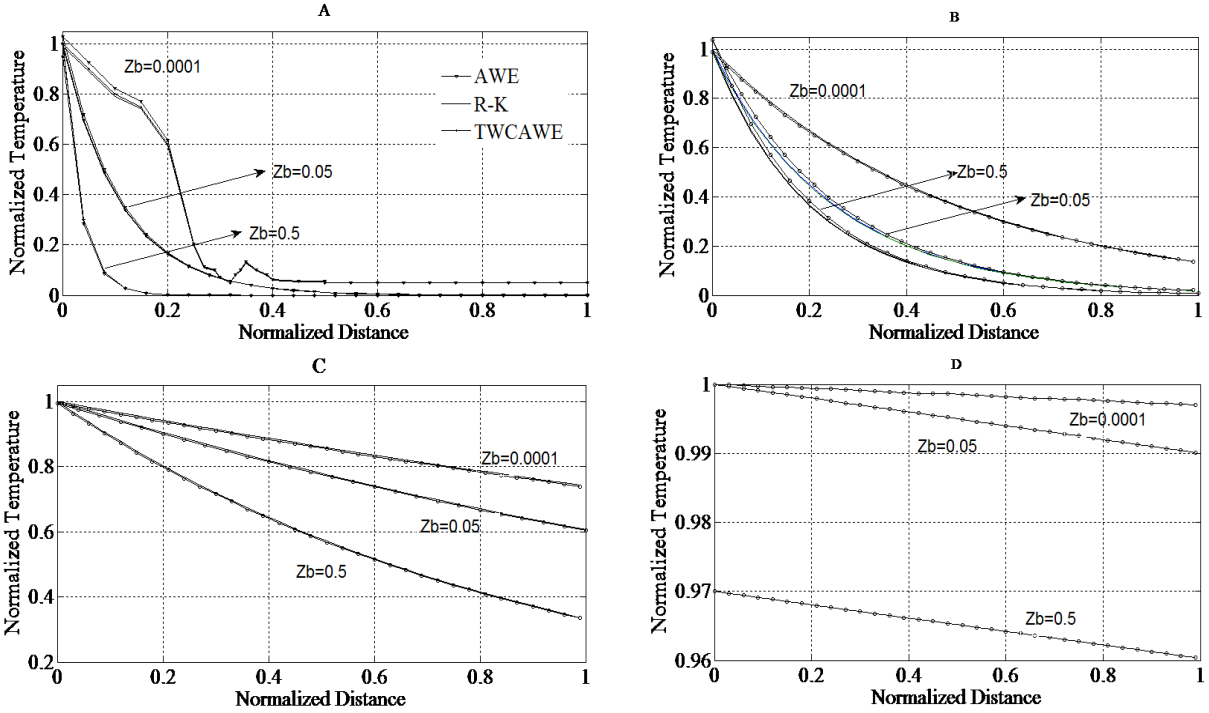

Figure 9. Normalized temperature distribution along centre of the slab for Z_b=0.5, 0.05 and Z_b=0.0001 with instantaneous heat imposed (a) at time 0.005 (b) at time 0.05 (c) at time 0.1 (d) at time 0.5

Table 2. Simulation time required by different method

Method Name	Time (s)	Ratio with respect to RK
Runge-Kutta	16	1
AWE	4.8	3.33
TWCAWE	4	4

Table 2 shows the computational time required by different method have been discussed in the present work. In these comparisons, we have used similar experimental settings of total length and width of the slab, total number of nodes, thermal conductivity and imposed temperature for the above mentioned methods. The TWCAWE technique is 4 times faster compared to RK and also 1.2 times faster than AWE.

4. Conclusion

In the present work, the heat conduction based on DPL has solved using FEM. The phase lag responsible for finite relaxation time that is varied to validate the capability of our proposed model for predicting the temperature responses in two-dimensional model. This work recommends the TWCAWE method to illustrate the non-Fourier heat conduction; there is no need to linearize the matrix equation and also no need to announce additional degree of freedom. . The numerical comparison presented in this work demonstrates that, TWCAWE method is precise and well-conditioned since this technique is able to approximate the delay and initial high frequencies precisely. Additionally, it is found that, TWCAWE is 1.2 times faster

than the ICAWE, but 4 times faster than the R-K. Moreover, the results are considerably superior than the ICAWE.

Acknowledgements

The work is founded by FP008-2014A, University Malaya, Malaysia.

References

[1] R. Quintanilla, R. Racke, "A note on stability in dual-phase-lag heat conduction", *International Journal of Heat and Mass Transfer*, vol. 49, no. 7, pp. 1209-1213, 2006.

[2] S. Rana, J. Kanesan, A. W. Reza, H. Ramiah, "Fast Transient Thermal Analysis of Non-Fourier Heat Conduction Using Tikhonov Well-Conditioned Asymptotic Waveform Evaluation", *The Scientific World Journal*, vol. 2014, Article ID 671619, 7 pages, 2014.

[3] J. S. Loh, I. A. Azid, K. N. Seetharamu, G. A Quadir, "Fast transient thermal analysis of Fourier and non-Fourier heat conduction", *International Journal of Heat and Mass Transfer*, vol. 50, no. 21, pp. 4400-4408, 2007.

[4] Y. Sun, I. S. Wichman, "On transient heat conduction in a one-dimensional composite slab", *International Journal of Heat and Mass* Transfer, vol. 47, no. 6, pp. 1555-1559, 2004.

[5] R. D. Slone, R. Lee, Jin-Fa Lee, "Well-conditioned asymptotic waveform evaluation for finite elements", *IEEE Transactions on Antennas and Propagation*, vol. 51, no. 9, pp. 2442-2447, 2003.

[6] R. D. Slone, R. Lee, Jin-Fa Lee, "Broadband model order reduction of polynomial matrix equations using single-point well-conditioned asymptotic waveform evaluation: derivations and theory", *International Journal for Numerical Methods in Engineering*, vol. 58, no. 15, pp. 2325-2342, 2003.

[7] S. Rana, J. Kanesan, A. W. Reza, H. Ramiah, "Tickhonov based well-condition asymptotic waveform evaluation for dual-phase-lag heat conduction", *Thermal Science*, vol. 18, pp. 1-12, 2014.

[8] S. Rana, J. Kanesan, H. Ramiah, A. W. Reza, "A wellcondition asymptotic waveform evaluation method for heat conduction problems", *Advanced Materials Research*, vol. 845, pp. 209-215, 2014.

[9] S. C. Mishra, H. Sahai, "Analysis of non-Fourier conduction and radiation in cylindrical medium using lattice Boltzmann method and finite volume method", *Int. J. Heat Mass Transfer*, vol. 61, pp. 41-55, 2013.

[10] A. Neumaier, "Solving ill-conditioned and singular linear system: a tutorial on regularization", *Siam Review*, vol. 40, no. 3, pp. 636-666, 1998.

[11] M. S. Lenzi, S. Lefteriu, H. Beriot, W. Desmet, "A fast frequency sweep approach using Pade approximations for solving Helmoltz finite element models", *Journal of Sound and Vibration*, vol. 332, no. 8, pp. 1897–1917, 2013.